ACS APPLIED MATERIALS & INTERFACES

Research Article

www.acsami.org

Characterization of the Mobility and Reactivity of Water Molecules on TiO_2 Nanoparticles by ^1H Solid-State Nuclear Magnetic Resonance

Lili Zhu,[†] Qiang Gu,[†] Pingchuan Sun,[‡] Wei Chen,[†] Xiaoliang Wang,*[,†] and Gi Xue*[,†]

[†]Department of Polymer Science and Engineering, School of Chemistry and Chemical Engineering, The State Key Laboratory of Coordination Chemistry, Nanjing University, Nanjing 210093, P. R. China

[‡]Key Laboratory of Functional Polymer Materials, Ministry of Education, Nankai University, Tianjin 300071, P. R. China

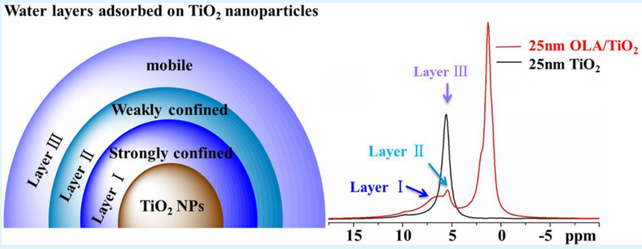

ABSTRACT: Understanding interfacial water behavior is essential to improving our understanding of the surface chemistry and interfacial properties of nanomaterials. Here using ^1H solid-state nuclear magnetic resonance (^1H SSNMR), we successfully monitored ligand exchange reaction between oleylamine (OLA) and adsorbed water on titanium dioxide nanoparticles (TiO_2 NPs). Three different types of interfacial waters with different reactivities were distinguished. The mobility of the adsorbed water molecules was characterized by dipolar filtered ^1H SSNMR. Our experimental results demonstrate that the adsorbed water can be categorized into three different layers: (i) rigid water species with restricted mobility closest to the surface of TiO_2 NPs, (ii) less mobile water species weakly confined on TiO_2 NPs, and (iii) water molecules with high mobility. Water in the third layer could be replaced by OLA, while water in the first and second layers remained intact. The finding that the interfacial water with the highest mobility has the strongest reactivity has guiding significance for tailoring the hydrophilic and hydrophobic properties of TiO_2 NPs.

KEYWORDS: *^1H solid-state NMR, interfacial water, TiO_2 nanoparticles*

■ INTRODUCTION

Water is a fascinating molecule that displays many unique and subtle properties.[1−6] The properties of water at interfaces are different from those of water in the bulk.[7−10] Recently, investigations about water on the surface of titanium dioxide (TiO_2), which is one of the most widely studied metal oxides among the various semiconductor materials,[11,12] have attracted the interest of researchers. The surface of TiO_2 usually adsorbs water molecules dissociatively to form surface hydroxyls, on which H_2O molecules are further adsorbed through hydrogen bonding. TiO_2 photocatalytic degradation of a variety of environmentally hazardous organic compounds has been extensively investigated, and it has been confirmed that the surface water plays an essential role in such interfacial chemical reactions.[13,14] Most investigations have been performed for the chemical species directly adsorbed on the surface after the evacuation of adsorbed water, assuming that the reactions occur directly on the solid surface. However, it should be mentioned that in practical applications the reactions usually take place under aerobic or aqueous conditions in the presence of adsorbed water, and the interfacial reactions can take place in adsorbed water regions. Therefore, a full understanding of the dynamics and chemical reactions of water at interfaces is of great significance. Although many studies about the interfacial behaviors of TiO_2 have been reported, only a few are focused on TiO_2 nanoparticles (NPs), mainly because the interface properties of nanoparticles are difficult to characterize.

Spectroscopic techniques, such as infrared spectroscopy (IR), Raman spectroscopy, nuclear magnetic resonance (NMR) spectroscopy, sum frequency generation (SFG), room-temperature matrix-isolation spectroscopy (RT-MIS), etc., have been proven to be efficient for characterizing the dynamics and reactions of water at the interface.[6−8,15−19] Among them, NMR spectroscopy has been utilized as one of the most effective techniques to investigate water adsorbed on solid surfaces.[16−18] Many NMR measurements of ligand-capped NPs were performed using liquid NMR, because nanoparticle suspensions in many aspects resemble true solutions and nanoparticles can have sufficient thermal energy to prevent sedimentation in solvents because of their small size.[20−27] However, the NMR peaks corresponding to the protons of the moieties closest to the surface are significantly broadened. The reasons for the peak broadening or resonance disappearance in liquid NMR spectra, which impedes an exact quantitative analysis, are still subject to discussion.[28−34] Studies have demonstrated that solid-state NMR (SSNMR) is an effective characterization technique for such immobilized systems.[13,14] Information about the interactions between surface hydroxyls groups and adsorbed molecules could be obtained by the analysis of line shape and relaxation times.[35−38] However, the technique has met with limited success because of the large proton line widths from homonuclear dipolar interactions that prevents identification of the different types of protons and their chemical shifts.

Received: August 16, 2013
Accepted: September 23, 2013
Published: September 23, 2013

dx.doi.org/10.1021/am403449j | *ACS Appl. Mater. Interfaces* 2013, 5, 10352−10356

In our previous studies, we demonstrated that by using fast magic angle spinning (MAS, spinning speed ν_R of >20 kHz) high-resolution ^{1}H SSNMR spectra of adsorbed species on nanoparticles could be obtained.[34,39−41] Moreover, we demonstrated that the 12-pulse dipolar filter experiment developed by Schmidt-Rohr et al.[28,29] can be utilized to investigate the mobility of adsorbed ligands on the surface of nanoparticles.[34,39−42] This method has been applied to distinguish a "mobile" component that has a dipolar interaction weaker than that of the rigid ones.[32,43]

In this work, we characterized water molecules adsorbed on TiO_2 NPs with different mobility and reactivity by ^{1}H SSNMR. Ligand exchange reactions between adsorbed water on the surface of TiO_2 NPs and free ligand oleylamine (OLA) were conducted. By ^{1}H SSNMR, the adsorption of OLA onto the surface of TiO_2 NPs was monitored and interfacial waters with different reactivities were distinguished. Dipolar filtered ^{1}H SSNMR detected the mobility of different interfacial water species and revealed the relationship between the mobility and reactivity of water.

EXPERIMENTAL SECTION

Materials. Titanium oxide TiO_2 nanopowder (25 and 100 nm) and oleylamine (technical grade 70%) were purchased from Sigma-Aldrich. The TiO_2 NPs were used after being treated with heat for 3 h at 150 °C. All of the solvents were commercially available and distilled before being used. All glassware was rinsed with copious amounts of ultrapure water and then dried in an oven prior to being used.

Synthesis of TiO_2 NPs Adsorbed with OLA and Water. OLA- and water-capped TiO_2 NPs were prepared by ligand exchange reaction between OLA and interfacial water. We mixed 20 mg of TiO_2 NPs (25 and 100 nm) with OLA in 50 mL of ethanol. After the mixture had been stirred for some time, the products were isolated by centrifugation and washed several times with ethanol. The resulting precipitate was dried in vacuum. The experimental parameters used to produce TiO_2 NPs with different adsorbed amounts of OLA are summarized in Table 1.

Table 1. Densities of OLA on TiO_2 NPs under Different Experimental Conditions

diameter of TiO_2 NPs (nm)	quality of TiO_2 NPs/OLA raw materials	reaction temperature (°C)	reaction time	mass faction of OLA (after reaction)	density (no. of chains/nm^2)
100	20 mg/20 mg	0	2 h	0.1	0.14
	20 mg/20 mg	0	2 h	0.5	0.80
	20 mg/60 mg	25	3 days	1	1.4
25	20 mg/60 mg	25	3 days	3	1.1

Instruments. After the ligand exchange reaction, the mass fraction of OLA was measured by means of thermogravimetric analysis (TGA) performed on a PerkinElmer Pyris 1 TGA instrument. Accurately weighed samples of 2−3 mg were run from room temperature to 700 °C at a rate of 20 °C/min under nitrogen (100 mL/min).

^{1}H SSNMR experiments were performed on a Varian Infinityplus-400 wide-bore (89 mm) NMR spectrometer at a proton frequency of 399.7 MHz. A 2.5 mm T3 double-resonance CPMAS probe was used for ^{1}H SSNMR experiments, and it can provide stable spinning up to 30 kHz within ±2 Hz using a zirconia PENCIL rotor. The magic angle spinning (MAS) frequency used in our experiments was 25 kHz. The 1H chemical shifts were referenced to external TMS. The 90° pulse width was 1.4 μs. Recycle delays between two scans were set to 6 s. The spectra were obtained with 32 scans for each spectrum. The background signal was separately collected under the same condition without sample and then subtracted from the spectra acquired with a sample to obtain all of the spectra used in the subsequent analysis. All of the NMR data were processed with Varian Spinsight software, and all experiments were conducted at room temperature. The temperature controller gas was on during for the entire experiment to keep the temperature at 30 ± 2 °C in the Varian Infinityplus-400 wide-bore (89 mm) NMR spectrometer.

One-dimensional liquid ^{1}H NMR spectra were recorded on an AV-400 NMR spectrometer (Bruker BioSpin, Coventy, U.K.), equipped with a 5 mm PABBO BB probe and operated at 400.13 MHz with a sample temperature of 25 °C.

RESULTS AND DISCUSSION

We used OLA as a compound to investigate ligand exchange reactions with the interfacial water and OLA. TiO_2 NPs adsorbed with different amounts of OLA were prepared by varying the experimental parameters (Table 1). Then NMR spectroscopy was utilized to monitor the reaction process and characterize the adsorbed species.

Figure 1 shows liquid NMR spectra of TiO_2 NPs co-adsorbed with water and oleylamine (OLA) in deuterated chloroform. For liquid NMR, there is always residual water in deuterated solvents that makes precise analysis of the NMR spectra difficult. However, liquid NMR spectroscopy is particularly informative for the ligand atoms remote from the core of NPs. NMR peaks of the methylene group at 1.4 ppm and the methyl group at 1.0 ppm from OLA can be observed in panels A and B of Figure 1. The resonances corresponding to the protons of the moiety closest to the surface are significantly broadened. This peak broadening or even disappearance in NMR spectra impedes an exact quantitative analysis. For adsorbed water on TiO_2 NPs, the chemical shift should be different from that of free water. However, in Figure 1, one cannot see the proton peak of water[16] upon binding to the TiO_2 NPs. The resonance for this part of the water was completely suppressed. We propose that some water molecules in the vicinity are immobilized, resulting in an inactive zone for liquid ^{1}H NMR measurement.

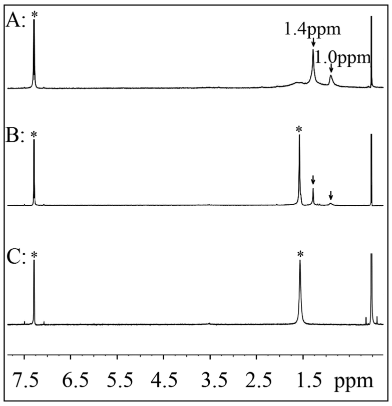

Figure 1. Liquid ^{1}H NMR in deuterated chloroform for (A) 100 nm TiO_2 NPs adsorbed with OLA (1.4 chains/nm^2), (B) 100 nm TiO_2 NPs adsorbed with OLA (0.14 chain/nm^2), and (C) TiO_2 NP raw material. Asterisks denote solvent peaks.

According to the spectra in Figure 1, liquid NMR is not suitable for our system. Therefore, we utilized ^{1}H SSNMR to characterize adsorbed species on TiO_2 NPs. For solid samples of nanoparticles, the parts of alkyl ligand remote from the core nanoparticle are flexible and NMR peaks with high resolution of these parts could be obtained. However, residual dipolar coupling broadens the signals of the protons closest to the surface bond, leaving only a featureless hump. The NMR signals for protons of adsorbed water on the suspended NPs were completely suppressed, as shown in the spectra of Figure 1. We recorded ^1H SSNMR spectra from the TiO_2 NPs adsorbed with water, by using fast MAS (ν_R = 25 kHz) to suppress line broadening caused by strong $^1H-^1H$ couplings and chemical shift anisotropy.[39,40] Figures 2 and 3 show ^1H SSNMR spectra for water molecules replaced by OLA on TiO_2 NPs with two different diameters. The ^1H SSNMR spectra were normalized to the quantity of samples.

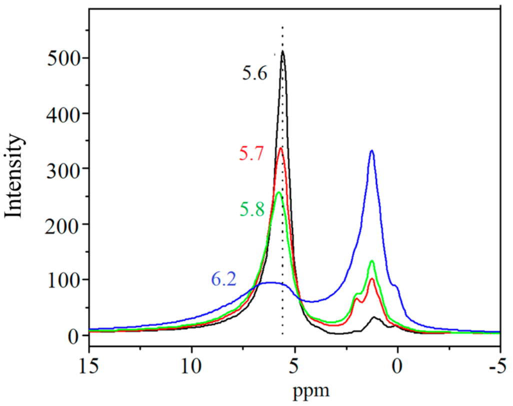

Figure 2. ^1H SSNMR spectra of water molecules on 100 nm TiO_2 NPs replaced by OLA at a ν_R of 25 kHz. The densities of OLA on TiO_2 NPs are 0 (black), 0.14 (red), 0.80 (green), and 1.40 chains/nm^2 (blue).

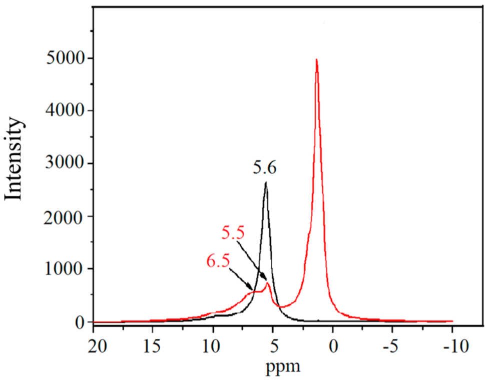

Figure 3. ^1H SSNMR spectra of water molecules on 25 nm TiO_2 NPs replaced by OLA at a ν_R of 25 kHz. The densities of OLA on TiO_2 NPs are 0 (black) and 1.1 chains/nm^2 (red).

As shown in Figure 2, 100 nm TiO_2 NPs showed a strong peak at 5.6 ppm that was assigned to the surface-adsorbed water molecules and a weak peak at ~1.2 ppm that was assigned to -CH_2 from the small amount of residual organic compounds on the untreated NPs. After the ligand exchange reactions, the intensity of the water peak decreased while that of -CH_2 increased, indicating the adsorbed water on the surface was gradually substituted with OLA. Meanwhile, for highly immobilized water near the surface region, the chemical shift of water moved to a low magnetic field and the signal became broader because of the reduced mobility.

The trend in the chemical shifts and line widths was more obvious with the reaction between OLA and the 25 nm TiO_2 NPs (Figure 3). The decrease in the intensity of the NMR peak at 5.6 ppm indicated the existence of mobile water that could be easily replaced by incoming OLA. Furthermore, according to the NMR signals in Figure 3, two different water species were clearly observed after the replacement; one is highly immobilized water, which showed broad NMR signals at 6.5 ppm, while the 5.5 ppm shift of the other is close to that of theTiO_2 NPs before ligand exchange (5.6 ppm). These two layers of water with different mobilities were further confirmed by the dipolar filtered ^1H SSNMR experiment. The difference in the ^1H SSNMR spectra between TiO_2 NPs with different diameters will be discussed later.

A dipolar filter ^1H experiment developed by Schmidt-Rohr et al.[39,40] was used to choose the ^1H magnetization with a weak dipole−dipole interaction. This method has also been applied to distinguish a "mobile" component that has dipolar interaction weaker than that of the rigid ones. As N_{cycle} increases in the dipolar filter experiment, the signals of the "rigid" parts are gradually suppressed, while the mobile component showed an isolated signal, as illustrated by the schematic diagram in Figure 4a. The faster the signal decays along N_{cycle}, the stronger the dipolar−dipolar interaction. Then, the mobilities of adsorbed OLA and water molecules were investigated by this dipolar filter ^1H SSNMR experiment. We compared the changes in integrated intensities of the measured NMR signals (in Figure 4b).

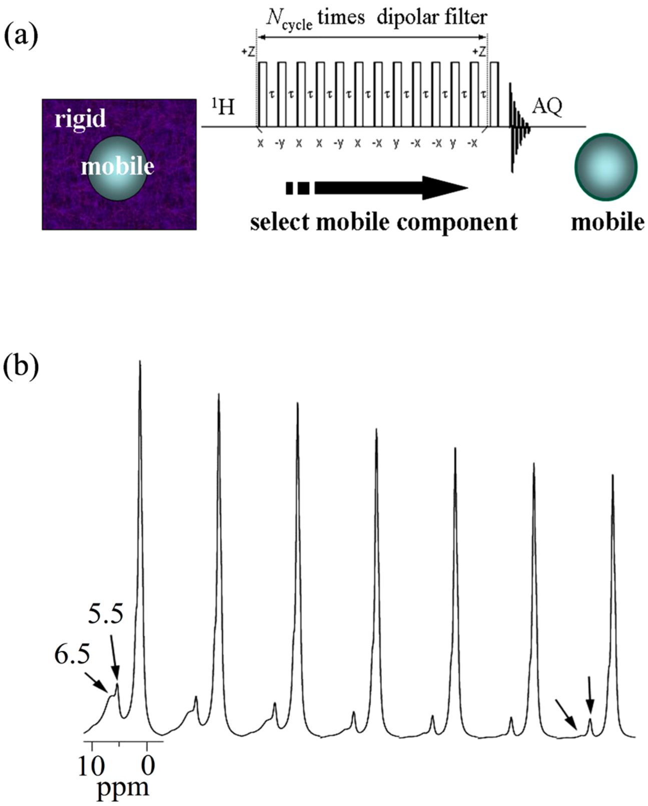

Figure 4. (a) Schematic diagram of detection of the mobile components with a dipolar filter. N_{cycle} indicates the multipulse dipolar filters.[17] (b) Dipolar filtered ^1H SSNMR spectra for water molecules on 25 nm TiO_2 NPs replaced with OLA.

The dipolar filtered ^1H SSNMR spectra for samples after the replacement reaction between OLA and water on 25 nm TiO_2 NPs show that there are three different kinds of co-adsorbed ligands. The intensity of the peak at 1.3 ppm for the methylene protons from OLA decayed slowly after N_{cycle} had reached 8 because of the flexibility of alkyl chains. Peaks at 6.5 and 5.5 ppm were assigned to different water species on TiO_2 NPs. The 6.5 ppm peak was suppressed almost completely, while the 5.5 ppm peak decayed much more slowly. The variation in intensity indicates that the mobility for water at 6.5 ppm is much lower than that at 5.5 ppm.

The mobility of adsorbed OLA molecules was characterized by a dipolar filter in ^1H SSNMR, as shown in Figure 5. In our previous studies, for a polymer/nanoparticle system[42] the larger the particle is, the stronger the confinement and the lower the mobility. In this system, the strong particle size dependence of ligand mobility was also confirmed. The signal of the -CH_2 protons for OLA on the 100 nm TiO_2 NPs decayed much faster than that on the 25 nm TiO_2 NPs, indicating the mobility of OLA adsorbed on larger TiO_2 nanoparticles is much higher than that on small nanoparticles. In this way, because of the stronger confinement between molecules and larger nanoparticles, the NMR signal for molecules on larger nanoparticles may be broader that on smaller ones (Figures 2 and 3). In Figure 3, for the 25 nm TiO_2 NPs with OLA (1.1 chains/nm^2), NMR signals at 5.5 and 6.5 ppm were observed. In Figure 2, for the 100 nm TiO_2 NPs with OLA (1.4 chains/nm^2), only a broad NMR signal attributed to the highly immobilized water at 6.2 ppm was observed and the NMR signals for the water with intermediate and high mobility around 5.5−5.6 ppm may overlap.

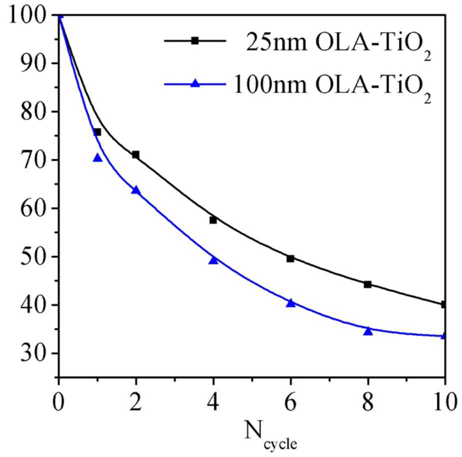

Figure 5. Integration NMR signals for -CH_2 protons vs N_{cycle} in dipolar filter ^1H SSNMR experiments for 25 (black) and 100 nm TiO_2 (blue) adsorbed on the surface.

Nosaka et al.[16,17] observed the variation of the ^1H NMR signals, including the line width, chemical shifts, and peak intensities, for water adsorbed on TiO_2 powders by increasing the experiment temperature. They proposed that the water region consists of three distinctly different water species with different mobilities. In this report, by designing ligand exchange reactions between interfacial water and incoming ligand OLA, we not only characterized the mobility of adsorbed water but also monitored the interfacial reactions on TiO_2 NPs. We found that the reactivity and mobility of adsorbed water are closely related. In addition, according to previous works,[16,17] the NMR signals of water on TiO_2 significantly changed with an increase in the NMR experimental temperature. In our experiment, the temperature controller gas was on during the entire experiment to keep the temperature at 30 ± 2 °C in the Varian Infinityplus-400 wide-bore (89 mm) NMR spectrometer. The sample maintained its original composition and property during the process of characterization. According to our experimental results, interfacial water that could be replaced by OLA has a higher mobility. Water that could not be replaced can be classified into two different groups with different mobilities. Thus, the adsorbed water on the surface of TiO_2 NPs can be categorized into three distinctly different water species (as illustrated in Scheme 1), comprising layer I (highly immobilized water that is strongly confined on the surface of TiO_2 NPs), layer II (relatively mobile water that is weakly confined), and layer III (mobile water that could be replaced by incoming ligands such as OLA). Water molecules in layer I and II are difficult to replace because of their affinity for the surface of TiO_2 NPs. Compared to that of the mobile water, the chemical shift of the rigid water shifted to a low magnetic field.

Scheme 1. Diagrams of Different Water Species Adsorbed on the Surface of TiO_2 NPs

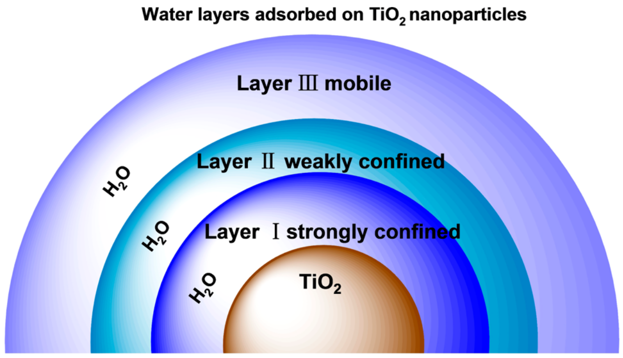

■ CONCLUSION

In this study, we characterized the interfacial ligand exchange reaction and the mobility of adsorbed water on the surface of TiO_2 NPs. The structures of all the surface species on TiO_2 NPs were characterized by ^1H SSNMR under magic angle spinning, while liquid NMR cannot detect immobilized water molecules on the surface of NPs. For the first time, we utilized the dipolar filter pulse sequence in ^1H SSNMR to investigate the mobility of water adsorbed on TiO_2 NPs. The experimental results revealed that the adsorbed water region can be categorized by three distinctively different states, comprising strongly confined rigid water, weakly confined relatively mobile water, and mobile water. The chemical shift of highly immobilized water moved to a low magnetic field, and the signal became even broader because of the reduced mobility. Mobile water is sensitively influenced by the surface environment, while water in the other two states is difficult to replace with incoming chemical compounds. Ligand exchange reaction is one of the best tools for modifying the surface of nanomaterials. The finding regarding the relation between the mobility and reactivity of ligands can probably be applied to all particle interfaces and thus can provide a clue about the design of nanodevices.

■ AUTHOR INFORMATION

Corresponding Authors

*E-mail: xuegi@nju.edu.cn.
*E-mail: wangxiaoliang@nju.edu.cn.

Notes

The authors declare no competing financial interest.

■ ACKNOWLEDGMENTS

We gratefully acknowledge National Basic Research Program of China (973 Program, 2012 CB 821503) and support from the National Natural Science Foundation of China (51133002, 21174062, 21274060, 21274059, and 21074052).

■ REFERENCES

(1) Fecko, C. J.; Eaves, J. D.; Loparo, J. J.; Tokmakoff, A.; Geissler, P. L. *Science* **2003**, *301*, 1698−1702.
(2) Luzar, A.; Chandler, D. *Nature* **1996**, *379*, 55−57.
(3) Auer, B. M.; Skinner, J. L. *J. Phys. Chem. B* **2009**, *113*, 4125−4130.
(4) Ishiyama, T.; Morita, A. *J. Phys. Chem. C* **2009**, *113*, 16299−16302.
(5) Jubb, A. M.; Hua, W.; Allen, H. C. *Acc. Chem. Res.* **2012**, *45*, 110−119.
(6) Shultz, M. J.; Vu, T. H.; Meyer, B.; Bisson, P. *Acc. Chem. Res.* **2012**, *45*, 15−22.
(7) Fayer, M. D. *Acc. Chem. Res.* **2012**, *45*, 3−14.
(8) Skinner, J. L.; Pieniazek, P. A.; Gruenbaum, S. M. *Acc. Chem. Res.* **2012**, *45*, 93−100.
(9) Berkowitz, M. L.; Vacha, R. *Acc. Chem. Res.* **2012**, *45*, 74−82.
(10) Roach, P.; Woodward, W.; Castleman, A.; Reber, A.; Khanna, S. *Science* **2009**, *323*, 492−495.
(11) Fujishima, A.; Honda, K. *Nature* **1972**, *238*, 37−38.
(12) Hoffmann, M. R.; Martin, S. T.; Choi, W. Y.; Bahnemann, D. W. *Chem. Rev.* **1995**, *95*, 69−96.
(13) Fox, M. A.; Dulay, M. T. *Chem. Rev.* **1993**, *93*, 341−357.
(14) Serpone, N.; Pelizzetti, E. *Photocatalysis: Fundamentals and Applications*; Wiley: New York, 1989.
(15) Finnie, K. S.; Cassidy, D. J.; Bartlett, J. R.; Woolfrey, J. L. *Langmuir* **2001**, *17*, 816−820.
(16) Nosaka, A. Y.; Nosaka, Y. *Bull. Chem. Soc. Jpn.* **2005**, *78*, 1595−1607.
(17) Nosaka, A. Y.; Fujiwara, T.; Yagi, H.; Akutsu, H.; Nosaka, Y. *J. Phys. Chem. B* **2004**, *108*, 9121−9125.
(18) Nosaka, A. Y.; Fujiwara, T.; Yagi, H.; Akutsu, H.; Nosaka, Y. *Langmuir* **2003**, *19*, 1935−1937.
(19) Zhu, L. L.; Zhang, C.; Guo, C. C.; Wang, X. L.; Sun, P. C.; Zhou, D. S.; Chen, W.; Xue, G. *J. Phys. Chem. C* **2013**, *117*, 11399−11404.
(20) Murray, R. W. *Chem. Rev.* **2008**, *108*, 2688−2720.
(21) Badia, A.; Demers, L.; Dickinson, L.; Morin, F. G.; Lennox, R. B.; Reven, L. *J. Am. Chem. Soc.* **1997**, *119*, 11104−11105.
(22) Fiurasek, P.; Reven, L. *Langmuir* **2007**, *23*, 2857−2866.
(23) Badia, A.; Singh, S.; Demers, L.; Cuccia, L.; Brown, G. R.; Lennox, R. B. *Chem.—Eur. J.* **1996**, *2*, 359−363.
(24) Hasan, M.; Bethell, D.; Brust, M. *J. Am. Chem. Soc.* **2002**, *124*, 1132−1133.
(25) Price, R. C.; Whetten, R. L. *J. Am. Chem. Soc.* **2005**, *127*, 13750−13751.
(26) Dorris, A.; Rucareanu, S.; Reven, L.; Barrett, C. J.; Lennox, R. B. *Langmuir* **2008**, *24*, 2532−2538.
(27) Milette, J.; Cowling, S. J.; Toader, V.; Lavigne, C.; Saez, I. M.; Lennox, R. B.; Goodby, J. W.; Reven, L. *Soft Matter* **2012**, *8*, 173−179.
(28) Schmidt-Rohr, K.; Spiess, H. W. *Multidimensional Solid-State NMR and Polymers*; Academic Press Inc.: San Diego, 1994.
(29) Egger, N.; Schmidt-Rohr, K.; Blumich, B.; Domke, W. D.; Stapp, B. *J. Appl. Polym. Sci.* **1992**, *44*, 289−295.
(30) Liu, Q. H.; Ma, C.; Hu, B. W.; Chen, Q.; Trebosc, J.; Lafon, O.; Amoureux, J. P. *J. Magn. Reson.* **2011**, *212*, 455−459.
(31) Calucci, L.; Forte, C.; Galleschi, L.; Geppi, M.; Ghiringhelli, S. *Int. J. Biol. Macromol.* **2003**, *32*, 179−189.
(32) Sun, P. C.; Dang, Q. Q.; Li, B. H.; Chen, T. H.; Wang, Y. N.; Lin, H.; Jin, Q. H.; Ding, D. T.; Shi, A. C. *Macromolecules* **2005**, *38*, 5654−5667.
(33) Guo, M. M. *Trends Polym. Sci.* **1996**, *4*, 238−244.
(34) Wang, X. L.; Gu, Q.; Sun, Q.; Zhou, D. S.; Sun, P. C.; Xue, G. *Macromolecules* **2007**, *40*, 9018−9025.
(35) Ladizhansky, V.; Hodes, G.; Vega, S. *J. Phys. Chem. B* **2000**, *104*, 1939−1943.
(36) Ueda, T.; Nakamura, N. *J. Phys. Chem. B* **2003**, *107*, 13681−13687.
(37) Enriquez, M. A.; Doremieuxmorin, C.; Fraissard, J. *Appl. Surf. Sci.* **1980**, *5*, 180−196.
(38) Turov, V. V.; Leboda, R.; Bogillo, V. I.; SkubiszewskaZieba, J. *J. Chem. Soc., Faraday Trans.* **1997**, *93*, 4047−4053.
(39) Gu, Q. A.; Wang, X. L.; Sun, P. C.; Zhou, D. S.; Xue, G. *Soft Matter* **2011**, *7*, 691−697.
(40) Han, J. L.; Zuo, C. W.; Gu, Q.; Li, D. W.; Wang, X. L.; Xue, G. *Appl. Surf. Sci.* **2008**, *255*, 2316−2321.
(41) Wang, X. L.; Tao, F. F.; Sun, P. C.; Zhou, D. S.; Wang, Z. Q.; Gu, Q.; Hu, J. L.; Xue, G. *Macromolecules* **2007**, *40*, 4736−4739.
(42) Zhu, L. L.; Wang, X. L.; Gu, Q.; Chen, W.; Sun, P. C.; Xue, G. *Macromolecules* **2013**, *46*, 2292−2297.
(43) Guo, M.; Zachmann, H. G. *Polymer* **1993**, *34*, 2503−2507.